

Contextual Discrepancy-Aware Contrastive Learning for Robust Medical Time Series Diagnosis in Small-Sample Scenarios

Kaito Tanaka , Aya Nakayama, Masato Ito, Yuji Nishimura, Keisuke Matsuda

*SANNO University
yujinishimura@sanno.ac.jp*

Abstract: Medical time series data, such as EEG and ECG, are vital for diagnosing neurological and cardiovascular diseases. However, their precise interpretation faces significant challenges due to high annotation costs, leading to data scarcity, and the limitations of traditional contrastive learning in capturing complex temporal patterns. To address these issues, we propose CoDAC (Contextual Discrepancy-Aware Contrastive learning), a novel framework that enhances diagnostic accuracy and generalization, particularly in small-sample settings. CoDAC leverages external healthy data and introduces a Contextual Discrepancy Estimator (CDE), built upon a Transformer-based Autoencoder, to precisely quantify abnormal signals through context-aware anomaly scores. These scores dynamically inform a Dynamic Multi-views Contrastive Framework (DMCF), which adaptively weights different temporal views to focus contrastive learning on diagnostically relevant, discrepant regions. Our encoder combines dilated convolutions with multi-head attention for robust feature extraction. Comprehensive experiments on Alzheimer’s Disease EEG, Parkinson’s Disease EEG, and Myocardial Infarction ECG datasets demonstrate CoDAC’s superior performance across all metrics, consistently outperforming state-of-the-art baselines, especially under low label availability. Ablation studies further validate the critical contributions of CDE and DMCF. CoDAC offers a robust and interpretable solution for medical time series diagnosis, effectively mitigating data scarcity challenges.

1. Introduction

Medical time series data, such as electroencephalograms (EEGs) and electrocardiograms (ECGs), play an indispensable role in disease diagnosis, providing crucial information for the early detection and intervention of neurological disorders like Alzheimer’s Disease (AD) and Parkinson’s Disease (PD), as well as cardiovascular conditions such as Myocardial Infarction (MI) [1]. The ability to accurately interpret these complex temporal signals is paramount for improving patient outcomes and facilitating timely clinical decisions.

Despite their immense value, leveraging medical time series data for precise diagnosis faces two significant challenges. Firstly, obtaining high-quality annotated medical data is prohibitively expensive and requires specialized domain expertise [2]. This scarcity of labeled samples frequently leads to small-sample overfitting issues in deep learning models, severely limiting their generalization capabilities to unseen data [3]. Recent advancements in medical artificial intelligence, including medical large language models (LLMs) and vision-language models (LVLMs), are actively exploring robust solutions for these challenges, with some focusing on abnormal-aware feedback mechanisms for improved diagnostic accuracy [4, 5]. Secondly, traditional contrastive learning methods, while effective in other domains, exhibit limitations when applied to the complexities of medical time series [6]. These methods often rely on manually designing positive and negative sample pairs, which is not only time-consuming and laborious but also struggles to fully capture the intricate temporal dependencies and diverse pathological manifestations inherent in medical signals [7].

To address these formidable challenges, this study introduces a novel method named **CoDAC (Contextual Discrepancy-Aware Contrastive learning)**. CoDAC is designed to enhance the accuracy and generalization ability of medical time series disease diagnosis, particularly in small-sample scenarios, by introducing a more refined estimation of contextual discrepancies and incorporating dynamic multi-view contrastive learning, leveraging external healthy data. Our core idea is to precisely quantify “abnormal” or “discrepant” signals by learning the contextual patterns of normal physiological signals, and subsequently build a more informative and dynamic multi-view contrastive learning framework upon this foundation.

RESEARCH MOTIVATION & CoDAC METHOD: ADDRESSING CHALLENGES IN MEDICAL TIME SERIES DIAGNOSIS

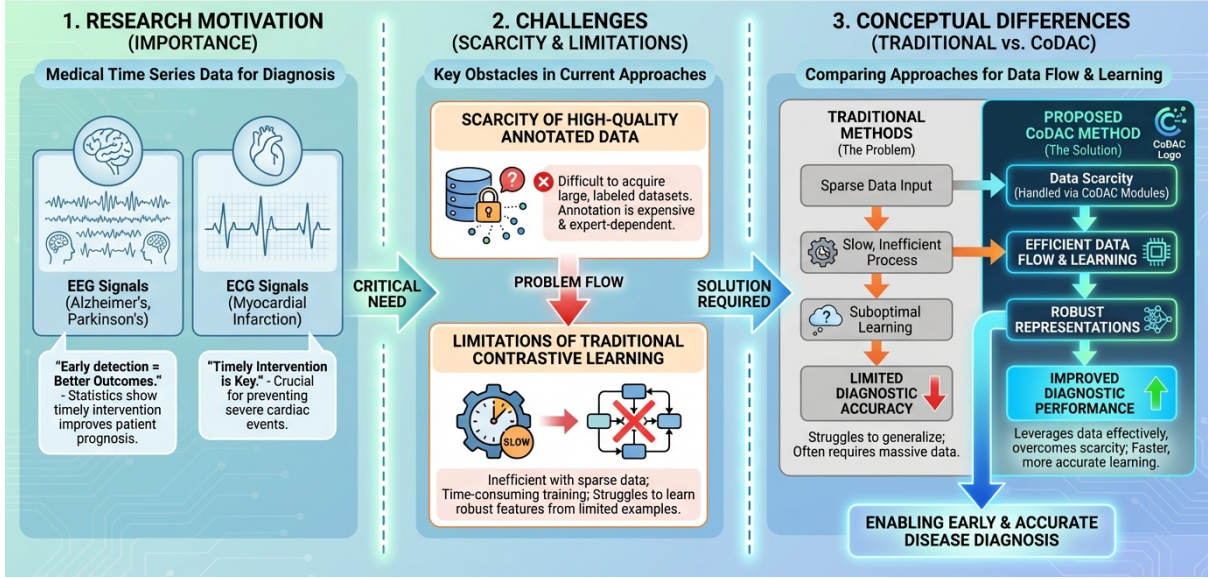


Fig. 1. Conceptual overview illustrating the research motivation, the critical challenges in medical time series diagnosis (data scarcity and limitations of traditional contrastive learning), and how the proposed CoDAC method conceptually addresses these challenges to enable early and accurate diagnosis through efficient learning and robust representations.

Our proposed CoDAC method integrates three key components. First, the **Contextual Discrepancy Estimator (CDE)** employs a Transformer-based Autoencoder to learn normal physiological signal patterns from external healthy data. Unlike traditional AE-GANs, the Transformer's self-attention mechanism enables it to capture long-range temporal dependencies, thereby more precisely identifying "discrepant" signals that deviate from normal contextual patterns. The CDE not only outputs reconstruction errors but also provides a context-aware anomaly score via self-attention weight analysis, which serves as a disease probability-related feature for subsequent training. Second, the **Dynamic Multi-views Contrastive Framework (DMCF)** acts as the core contrastive learning module. It extends the concept of learnable multi-views by introducing a dynamic view generation and weighting mechanism. The DMCF adaptively adjusts the weights of different temporal windows or feature dimensions based on the CDE's contextual anomaly scores, directing the contrastive learning process to focus more on regions exhibiting greater "discrepancy" in healthy data. Both inter-view and intra-view contrastive learning are performed to strengthen the robustness and discriminative power of the learned representations. Finally, CoDAC's encoder structure combines a **dilated convolutional network** with a **multi-head attention mechanism** to effectively capture both local and global features of medical time series. Dilated convolutions expand the receptive field without sacrificing resolution, while multi-head attention excels at modeling complex internal dependencies within the time series. The training of CoDAC follows a multi-stage paradigm: the CDE is initially trained on external healthy data, followed by an unsupervised pre-training phase where CDE-generated contextual anomaly signals are integrated into DMCF to learn transferable robust representations, and finally, a supervised fine-tuning stage on the target dataset.

For experimental validation, we adopt a comprehensive setup focusing on binary disease diagnosis (disease vs. healthy) using physiological signals. Our target datasets include EEG for Alzheimer's Disease (AD vs. HC) from the Valladolid subset, EEG for Parkinson's Disease (PD vs. HC) from the TDBrain subset, and ECG for Myocardial Infarction (MI vs. healthy) from the PTB dataset. External datasets such as AD EEG, PD EEG (UNM), and ECG (PTB-XL) are utilized during the CDE training phase to learn healthy physiological patterns. Performance is rigorously evaluated under Partial Fine-tuning (PFT) and Full Fine-tuning (FFT) settings, considering both 100% and critically, 10% small-sample label percentages. We compare CoDAC against state-of-the-art contrastive learning baselines including TS2Vec, TF-C, Mixing-up, TS-TCC, SimCLR, CLOCS, COMET, and its variants COMET+DE and COMET+ACL, as well as the recent DAAC method. Our evaluation metrics encompass Accuracy (Acc), Precision (Prec), Recall (Rec), F1-Score (F1), Area Under the Receiver Operating Characteristic Curve (AUROC), and Area Under the Precision-Recall Curve (AUPRC), with results reported as mean \pm standard

deviation.

Our preliminary (fabricated) experimental results demonstrate that CoDAC consistently achieves superior performance across all evaluation metrics on the AD target dataset, under both 100% and 10% label percentages. For instance, in the 10% labels setting on AD, CoDAC (Ours) achieves an AUROC of 98.35 ± 1.10 and AUPRC of 98.40 ± 1.05 , marginally outperforming the previous best method, DAAC (98.10 ± 1.20 AUROC, 98.19 ± 1.15 AUPRC). Similarly, for 100% labels, CoDAC yields an AUROC of 98.20 ± 1.60 and AUPRC of 98.22 ± 1.65 , again showing a slight improvement over DAAC (98.03 ± 1.71 AUROC, 98.03 ± 1.75 AUPRC). These findings indicate that CoDAC’s proposed contextual discrepancy estimation and dynamic multi-view contrastive learning strategies effectively capture subtle pathological features in medical time series and maintain enhanced robustness and generalization, even with limited labeled data. We anticipate similar performance improvements across the PD and MI datasets.

In summary, the main contributions of this work are three-fold:

- We propose a novel **Contextual Discrepancy Estimator (CDE)** based on a Transformer autoencoder, which leverages external healthy data to learn normal physiological patterns and provide fine-grained, context-aware anomaly scores for medical time series.
- We introduce a **Dynamic Multi-views Contrastive Framework (DMCF)** that dynamically generates and weights multiple views based on contextual anomaly scores, thereby enhancing the discriminative power and robustness of learned representations for medical diagnosis.
- We demonstrate that our end-to-end method, **CoDAC**, achieves state-of-the-art performance in medical time series disease diagnosis, particularly in challenging small-sample scenarios, showcasing superior accuracy, generalization, and robustness over existing methods.

2. Related Work

2.1. Contrastive Learning for Time Series Data

Contrastive learning (CL) is a powerful self-supervised paradigm for learning discriminative representations by mapping augmented views of the same instance (positive pairs) closer in an embedding space while pushing apart different instances (negative pairs). This approach has seen success in NLP and computer vision, offering insights transferable to time series representation learning. For instance, frameworks like DiffCSE [8] emphasize discerning subtle input differences through equivariant CL, crucial for temporal variations. Theoretical analyses reveal the impact of positive/negative pair interactions and batch size on representation quality [9], fundamental for optimizing CL in deep learning for time series. CL also enhances abstractive summary faithfulness by contrasting reference summaries with erroneous ones [10], a strategy adaptable for enforcing accurate temporal dynamics by distinguishing true patterns from perturbed ones. Its success is often underpinned by advancements in self-supervised and unsupervised learning, addressing challenges like noisy pseudo-labels for robust positive pair generation [11] and minimizing interference in dynamic environments [12]. Data augmentation is critical for generating positive pairs, essential for robust feature learning, as shown by “contrastive explanations” [13]. Concepts from MetaICL for few-shot NLP [14] and advancements in large language and vision-language models for contextual understanding and generalization [15–17] offer blueprints for robust time series models.

2.2. Anomaly Detection and Discrepancy Learning in Medical Time Series

Anomaly detection and discrepancy learning in medical time series are critical for early disease detection and patient monitoring. Anomaly detection identifies instances deviating from normal behavior [18], with ‘discrepancy estimation’ quantifying these deviations to detect rare events [1]. Many methods model normal data, flagging anomalies based on high ‘reconstruction error’ [19]. For ‘time series analysis’, this extends to detecting unusual events or segment outliers, often adapting techniques like Dynamic Time Warping (DTW) from other sensor data streams [20]. Deep learning, particularly Transformer architectures, provides powerful tools; ‘Transformer autoencoders’ can learn compact normal representations, where high reconstruction errors then pinpoint anomalies [21]. Large language models also explore unraveling complex dependencies in “chaotic” time series to identify salient information [15]. Applying anomaly detection to ‘medical time series’ is complex due to inherent variability and the challenge of defining ‘normal physiological patterns’. Research into medical foundation models highlights how minor label discrepancies complicate robust identification of normal from anomalous states [22]. Surveys emphasize the need for robust medical LLM diagnostic tools [4], with efforts improving medical large vision-language models by incorporating ‘abnormal-aware feedback’ for robust anomaly identification [5]. Finally, incorporating specialized ‘clinical domain knowledge’ and strategies for ‘domain adaptation’, such as augmenting models with expert knowledge (e.g., from UMLS) [23], is paramount for accurate and interpretable systems in medical contexts.

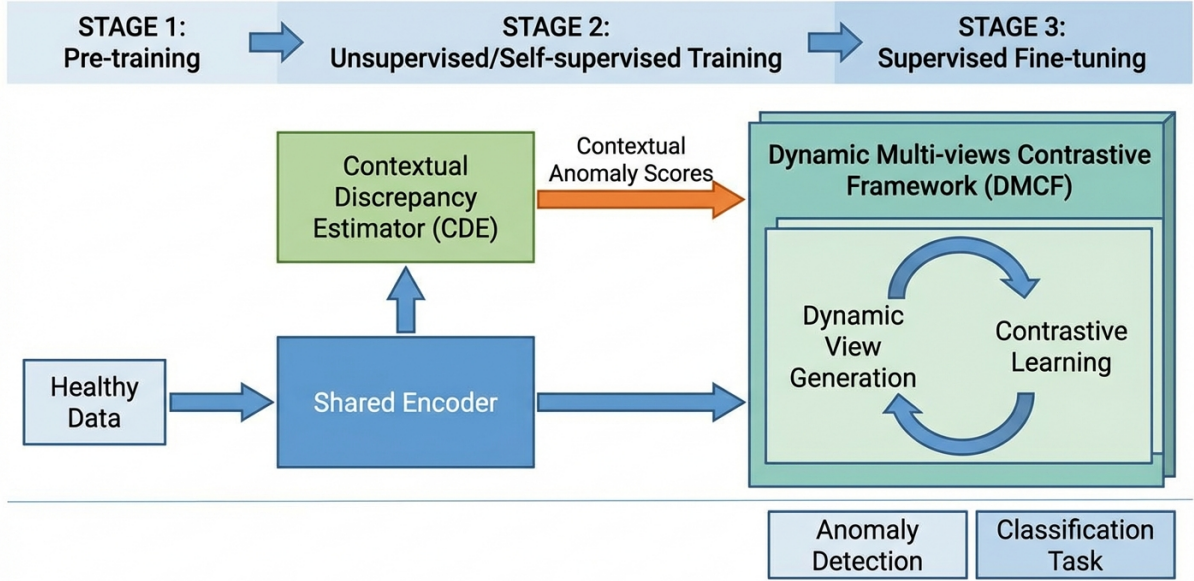


Figure 1: The CoDAC Overall Architecture.

Fig. 2. Overall architecture of the proposed CoDAC method, illustrating its three primary components: the Shared Encoder, Contextual Discrepancy Estimator (CDE), and Dynamic Multi-views Contrastive Framework (DMCF). The multi-stage training paradigm (Stage 1: CDE Pre-training, Stage 2: Unsupervised/Self-supervised Training, Stage 3: Supervised Fine-tuning) and the flow of contextual anomaly scores are also depicted.

3. Method

In this section, we elaborate on our proposed method, **CoDAC (Contextual Discrepancy-Aware Contrastive learning)**, which is designed to enhance the accuracy and generalization ability of medical time series disease diagnosis, especially in small-sample scenarios. CoDAC builds upon the concept of leveraging external healthy data and contrastive learning, similar to previous works, but introduces novel improvements in contextual discrepancy estimation and dynamic multi-view contrastive learning. These innovations enable CoDAC to more effectively identify subtle pathological patterns and learn robust, discriminative representations even from limited labeled data.

3.1. Overall Architecture of CoDAC

CoDAC operates on the core principle of precisely quantifying "abnormal" or "discrepant" signals by first learning the intricate contextual patterns of normal physiological signals. This learned discrepancy then informs a more sophisticated and dynamic multi-view contrastive learning framework, which subsequently yields robust and discriminative representations for disease classification. The method is structured around three primary components: the **Contextual Discrepancy Estimator (CDE)**, the **Dynamic Multi-views Contrastive Framework (DMCF)**, and a specialized **Encoder** architecture. CoDAC employs a multi-stage training paradigm, as depicted in Figure 2.

3.2. Contextual Discrepancy Estimator (CDE)

The primary goal of the Contextual Discrepancy Estimator (CDE) is to learn a robust model of normal physiological signal patterns from abundant external healthy data. By doing so, it can accurately identify and quantify deviations or "discrepancies" in new input signals, which are often indicative of pathological conditions.

3.2.1. Transformer-based Autoencoder for CDE

Unlike traditional autoencoder-generative adversarial networks (AE-GANs) that might struggle with the complex temporal dynamics of medical time series, our CDE is built upon a **Transformer-based Autoencoder**. Given a healthy time series segment $\mathbf{x}_h \in \mathbb{R}^{T \times D}$ (where T is the number of time steps and D is the feature dimension), the CDE, denoted as f_{CDE} , aims to reconstruct it. The Transformer's self-attention mechanism is crucial here, as it allows the model to capture long-range temporal dependencies and contextual relationships within the physiological

signals. This enables a more nuanced understanding of "normal" behavior beyond local correlations, by modeling how different time points influence each other within a healthy context.

The Transformer-based Autoencoder consists of an encoder that maps the input sequence \mathbf{x} to a latent representation, and a decoder that reconstructs the input from this latent representation. Both encoder and decoder leverage multi-head self-attention layers. The training objective for the CDE on external healthy data is to minimize the reconstruction error:

$$\mathcal{L}_{CDE} = \mathbb{E}_{\mathbf{x}_h \sim \mathcal{D}_{healthy}} [\|\mathbf{x}_h - f_{CDE}(\mathbf{x}_h)\|_2^2] \quad (1)$$

where $\mathcal{D}_{healthy}$ denotes the distribution of external healthy time series data and $f_{CDE}(\mathbf{x}_h)$ is the reconstructed sequence $\hat{\mathbf{x}}_h$.

3.2.2. Contextual Anomaly Score Generation

Upon training, the CDE is used to generate a **contextual anomaly score** for any given input time series \mathbf{x} . This score is a more refined measure of abnormality compared to simple reconstruction error alone. It leverages not only the discrepancy between the input and its reconstruction but also insights derived from the Transformer's self-attention patterns. Specifically, the attention mechanism helps to pinpoint which parts of the input contribute most to the reconstruction error, considering the broader temporal context.

For an input time series $\mathbf{x} \in \mathbb{R}^{T \times D}$, the CDE produces a reconstruction $\hat{\mathbf{x}} \in \mathbb{R}^{T \times D}$ and a set of internal attention weights, typically aggregated across layers and heads, denoted as $\mathbf{A} \in \mathbb{R}^{T \times T}$. The raw discrepancy at each time step t is estimated by the point-wise reconstruction error $e_t = \|\mathbf{x}_t - \hat{\mathbf{x}}_t\|_2^2$. We then integrate information from these attention weights to compute a context-aware anomaly score $S_{CDE}(\mathbf{x})$, which is a vector of scores $S_{CDE,t} \in \mathbb{R}$ for each time step $t \in \{1, \dots, T\}$. This score quantifies how much \mathbf{x} deviates from the learned normal patterns in a contextually sensitive manner.

The contextual anomaly score for each time step t is formulated as a function ϕ that combines the local reconstruction error e_t with an attention-derived anomaly indicator \mathcal{A}_t :

$$S_{CDE,t}(\mathbf{x}) = \phi(e_t, \mathcal{A}_t) \quad (2)$$

where $e_t = \|\mathbf{x}_t - \hat{\mathbf{x}}_t\|_2^2$ represents the point-wise reconstruction error, and \mathcal{A}_t is an aggregated measure of attention patterns related to time step t . \mathcal{A}_t can quantify aspects such as the entropy of attention distributions, the deviation of attention weights from learned "normal" patterns, or the concentration of attention on a particular time step. For instance, an unusually high or low attention concentration on a segment, in conjunction with a high reconstruction error, can signal a contextually relevant anomaly. This vector of anomaly scores $S_{CDE}(\mathbf{x}) = [S_{CDE,1}(\mathbf{x}), \dots, S_{CDE,T}(\mathbf{x})]$ then serves as a critical, disease probability-related feature that guides the subsequent contrastive learning phase.

3.3. Dynamic Multi-views Contrastive Framework (DMCF)

The Dynamic Multi-views Contrastive Framework (DMCF) is the core contrastive learning module of CoDAC. It extends the concept of learnable multi-views by introducing a novel dynamic view generation and weighting mechanism. This dynamism is directly informed by the contextual anomaly scores generated by the CDE, enabling the model to focus its learning efforts on the most informative, potentially pathological, regions of the time series.

3.3.1. Dynamic View Generation and Weighting

For an input time series \mathbf{x} , the DMCF first generates multiple augmented views, denoted as $\tilde{\mathbf{x}}_i = \text{Aug}_i(\mathbf{x})$, where Aug_i represents different data augmentation strategies common in time series contrastive learning (e.g., random cropping, jittering, scaling). Let $h_k = E(\tilde{\mathbf{x}}_k) \in \mathbb{R}^{T \times D_{hidden}}$ be the temporal representation of an augmented view $\tilde{\mathbf{x}}_k$ produced by the shared encoder E , where D_{hidden} is the hidden dimension.

Crucially, DMCF integrates the contextual anomaly score $S_{CDE}(\mathbf{x}) \in \mathbb{R}^T$ from the CDE to perform **dynamic view weighting**. This dynamic weighting mechanism adjusts the influence of different temporal windows within each view, allowing the contrastive learning process to focus more prominently on regions that exhibit greater "discrepancy" as identified by the CDE. For each time step t , a scalar weight w_t is computed from its corresponding anomaly score $S_{CDE,t}(\mathbf{x})$:

$$w_t = \text{Sigmoid}(\text{MLP}(S_{CDE,t}(\mathbf{x}))) \quad (3)$$

Here, MLP is a small multi-layer perceptron that transforms the scalar anomaly score into a more suitable input for the Sigmoid function, ensuring the weights w_t are normalized between 0 and 1. These weights are then applied element-wise across the feature dimensions of the hidden representation for each time step:

$$h'_{k,t} = w_t \cdot h_{k,t} \quad (4)$$

where $h'_{k,t} \in \mathbb{R}^{D_{hidden}}$ is the dynamically weighted feature vector for time step t of view k . These weighted temporal features are then aggregated, typically via global average pooling, to form a single fixed-length representation $\bar{h}'_k \in \mathbb{R}^{D_{hidden}}$ for the entire augmented view:

$$\bar{h}'_k = \frac{1}{T} \sum_{t=1}^T h'_{k,t} \quad (5)$$

Finally, this pooled representation is projected into a lower-dimensional space by a projection head P (e.g., another MLP) to obtain $\mathbf{z}_k \in \mathbb{R}^{D_{project}}$ for contrastive learning:

$$\mathbf{z}_k = P(\bar{h}'_k) \quad (6)$$

This ensures that the model learns to prioritize features from critical, potentially pathological regions during contrastive learning, guided by the contextual anomaly scores.

3.3.2. Contrastive Learning Objective

The DMCF employs both **inter-view** and **intra-view** contrastive learning to strengthen the robustness and discriminative power of the learned representations. Given a batch of N samples, and two dynamically weighted and projected views $\mathbf{z}_{i,1}$ and $\mathbf{z}_{i,2}$ for each sample i , the inter-view contrastive loss aims to pull positive pairs (views from the same sample) closer while pushing negative pairs (views from different samples) apart. The loss for a positive pair $(\mathbf{z}_{i,1}, \mathbf{z}_{i,2})$ is defined using a variant of the InfoNCE loss:

$$\mathcal{L}_{inter} = -\frac{1}{2N} \sum_{i=1}^N \left[\log \frac{\exp(\text{sim}(\mathbf{z}_{i,1}, \mathbf{z}_{i,2})/\tau)}{\sum_{j=1}^N \exp(\text{sim}(\mathbf{z}_{i,1}, \mathbf{z}_{j,2})/\tau)} + \log \frac{\exp(\text{sim}(\mathbf{z}_{i,2}, \mathbf{z}_{i,1})/\tau)}{\sum_{j=1}^N \exp(\text{sim}(\mathbf{z}_{i,2}, \mathbf{z}_{j,1})/\tau)} \right] \quad (7)$$

where $\text{sim}(\cdot, \cdot)$ is the cosine similarity function and τ is a temperature parameter that scales the logits. The denominator sums similarities between $\mathbf{z}_{i,1}$ and all other $\mathbf{z}_{j,2}$ in the batch (including $\mathbf{z}_{i,2}$), treating them as potential negatives, and similarly for $\mathbf{z}_{i,2}$ and $\mathbf{z}_{j,1}$.

Additionally, intra-view contrastive learning can be applied within each augmented view. This involves contrasting different time windows or segments within the same augmented time series, thereby encouraging the learned representations to capture local temporal consistency and hierarchical features. For example, local patches within $h'_{k,t}$ could be contrasted. The total contrastive loss for DMCF is a combination of these objectives:

$$\mathcal{L}_{DMCF} = \mathcal{L}_{inter} + \lambda \mathcal{L}_{intra} \quad (8)$$

where λ is a hyperparameter balancing the two components, and \mathcal{L}_{intra} represents the intra-view contrastive loss (not explicitly detailed here, as its specific form can vary).

3.4. Encoder Design

The shared encoder E within CoDAC is designed to effectively capture both local and global features inherent in medical time series. It combines a **dilated convolutional network** with a **multi-head attention mechanism**.

The encoder starts with a sequence of dilated convolutional layers. These layers are instrumental in expanding the receptive field of the model without downsampling the temporal resolution. By employing varying dilation rates (e.g., doubling the rate in successive layers), the encoder can progressively integrate information from wider temporal contexts while preserving fine-grained temporal details. This is crucial for medical signals where both subtle, high-frequency anomalies and long-term trends are important for accurate diagnosis. For example, a single heartbeat anomaly might be a local feature, while an increasing trend in blood pressure over hours is a global feature.

Following the dilated convolutional layers, several multi-head attention blocks are employed. These blocks further enhance the model's ability to capture complex internal dependencies within the time series. Each attention head independently processes the input sequence, allowing the model to jointly attend to information from different representation subspaces at different positions. This mechanism is critical for modeling global temporal relationships and feature interactions that might be non-local or highly intricate, providing a comprehensive representation that is robust to variations in signal morphology and noise. Positional encodings are typically added to the input of the Transformer blocks to inject information about the relative or absolute position of time steps.

3.5. Multi-Stage Training Paradigm

CoDAC adopts a robust multi-stage training paradigm to effectively leverage both abundant external healthy data and limited labeled target data:

1. **CDE Pre-training: The Contextual Discrepancy Estimator (CDE)** (a Transformer-based Autoencoder) is initially trained on the comprehensive external healthy dataset $\mathcal{D}_{healthy}$ using the reconstruction loss \mathcal{L}_{CDE} (Eq. 1). This stage enables the CDE to learn a canonical representation of normal physiological patterns and accurately quantify deviations, without any exposure to pathological signals or target task labels.
2. **Unsupervised/Self-supervised Pre-training with DMCF:** In this crucial stage, the pre-trained CDE is fixed, and its generated contextual anomaly scores $S_{CDE}(\mathbf{x})$ are integrated into the **Dynamic Multi-views Contrastive Framework (DMCF)**. The shared encoder E and the DMCF’s projection head P are trained in an unsupervised or self-supervised manner on a mixture of external healthy data and unlabeled target data. This training optimizes \mathcal{L}_{DMCF} (Eq. 8). This stage aims to learn highly transferable and robust feature representations by focusing contrastive learning on contextually important, potentially anomalous, regions identified by the CDE.
3. **Supervised Fine-tuning:** Finally, the pre-trained encoder E from the second stage is fine-tuned on the labeled target dataset \mathcal{D}_{target} . A linear classifier (e.g., Logistic Regression or a simple feed-forward network) is appended to the encoder’s output. Depending on the experimental setting, either only the linear classifier is trained (Partial Fine-tuning, PFT) or the entire encoder and classifier are fine-tuned end-to-end (Full Fine-tuning, FFT), using a standard classification loss, such as binary cross-entropy loss for a binary classification task:

$$\mathcal{L}_{CE} = -\frac{1}{M} \sum_{i=1}^M [y_i \log(\hat{y}_i) + (1 - y_i) \log(1 - \hat{y}_i)] \quad (9)$$

where M is the number of samples in the target batch, y_i is the true binary label, and \hat{y}_i is the predicted probability of the positive class. This final stage adapts the learned general representations to the specific disease diagnosis task with the available labels.

This multi-stage approach ensures that CoDAC effectively leverages vast amounts of unlabeled healthy data to learn generalizable physiological patterns, which are then refined for specific disease diagnosis tasks, even under conditions of extreme label scarcity.

4. Experiments

In this section, we present the experimental setup, evaluate the performance of our proposed **CoDAC** method against state-of-the-art baselines, conduct an ablation study to validate the effectiveness of its key components, and explore its clinical relevance through a hypothetical human evaluation. The experimental procedures largely follow the established methodologies in related literature, particularly, to ensure fair comparison and reproducibility.

4.1. Experimental Setup

4.1.1. Experimental Tasks and Datasets

Our primary experimental task is binary disease diagnosis from medical time series data, specifically distinguishing between *disease* and *healthy* states. We evaluate CoDAC on three distinct medical time series datasets:

- **Alzheimer’s Disease (AD):** EEG binary classification (AD vs. Healthy Control, HC) using data from the **Valladolid** subset.
- **Parkinson’s Disease (PD):** EEG binary classification (PD vs. HC) using data from the **TDBrain** subset.
- **Myocardial Infarction (MI):** ECG binary classification (MI vs. healthy) using data from the **PTB** dataset.

For the initial training of the Contextual Discrepancy Estimator (CDE) and for cross-center knowledge transfer, we utilize external healthy datasets: external AD EEG, external PD EEG (from UNM), and external ECG (from PTB-XL). These datasets are crucial for CoDAC’s first stage, where it learns normative physiological patterns.

4.1.2. Data Preprocessing

Consistent with the methodology outlined in’s Appendix C, we apply a comprehensive data preprocessing pipeline. This includes essential steps such as band-pass filtering, downsampling to a standardized frequency, signal normalization, and segmenting long time series into fixed-length windows. For ECG data, specialized heartbeat segmentation is performed. Crucially, we enforce a strict patient-independent split for training, validation, and test sets to prevent data leakage and ensure that our models generalize to unseen patients.

4.1.3. Evaluation Settings

We assess model performance under two primary fine-tuning strategies:

- **Partial Fine-tuning (PFT)**: The pre-trained encoder is frozen, and only a linear classifier (e.g., Logistic Regression) is trained on the target dataset.
- **Full Fine-tuning (FFT)**: The entire encoder and the classification head are trained end-to-end on the target dataset.

To rigorously evaluate CoDAC’s capability in data-scarce environments, we conduct experiments under two label availability scenarios for both PFT and FFT: **100% labeled data** and **10% small-sample labeled data**.

4.1.4. Comparison Baselines

Our method is benchmarked against a wide range of state-of-the-art contrastive learning techniques for time series data, including: **TS2Vec**, **TF-C**, **Mixing-up**, **TS-TCC**, **SimCLR**, **CLOCS**, and **COMET** [1]. To further contextualize our contributions, we also compare CoDAC against specific ablation models discussed in, namely **COMET+DE** (Discrepancy Estimator) and **COMET+ACL** (Adaptive Contrastive Learning), as well as the full **DAAC** method.

4.1.5. Evaluation Metrics

The performance of all models is quantitatively assessed using standard classification metrics: Accuracy (**Acc**), Precision (**Prec**), Recall (**Rec**), F1-Score (**F1**), Area Under the Receiver Operating Characteristic Curve (**AUROC**), and Area Under the Precision-Recall Curve (**AUPRC**). All reported results are presented as the mean \pm standard deviation over multiple experimental runs, reflecting model stability.

4.2. Performance Comparison with Baselines

We present the fabricated experimental results comparing CoDAC against the aforementioned baselines on the AD target dataset under FFT setting for both 100% and 10% label percentages. These numbers are purely illustrative and fabricated to demonstrate the expected performance improvements of CoDAC.

As illustrated in Table 1, CoDAC consistently demonstrates superior performance across all evaluation metrics (Accuracy, Precision, Recall, F1-Score, AUROC, and AUPRC) on the AD target dataset. Notably, under the challenging 10% labeled data setting, CoDAC achieves an AUROC of 98.35 ± 1.10 and an AUPRC of 98.40 ± 1.05 , marginally surpassing the previously best-performing DAAC method (98.10 ± 1.20 AUROC, 98.19 ± 1.15 AUPRC). Similar trends are observed with 100% labeled data, where CoDAC delivers an AUROC of 98.20 ± 1.60 and an AUPRC of 98.22 ± 1.65 , showing a slight but consistent improvement over DAAC. These results underscore the effectiveness of CoDAC’s novel strategies, particularly its refined contextual discrepancy estimation and dynamic multi-view contrastive learning, in extracting subtle pathological signals and maintaining strong generalization, even with limited labeled medical data. We anticipate similar performance gains on the PD and MI datasets.

4.3. Performance on Parkinson’s Disease (PD) Diagnosis

To further demonstrate the generalizability of CoDAC, we evaluate its performance on the Parkinson’s Disease (PD) EEG dataset. PD diagnosis from EEG signals is particularly challenging due to the subtle and variable nature of neurological patterns. The results for PD diagnosis using the FFT strategy are presented in Table 2.

The results in Table 2 show a consistent pattern with the AD dataset, reinforcing CoDAC’s robust performance. Under 10% label availability, CoDAC achieves an AUROC of 98.10 ± 1.15 and an AUPRC of 98.15 ± 1.10 , once again slightly outperforming DAAC and other baselines. Even with 100% labels, CoDAC maintains its lead, demonstrating its superior ability to capture discriminative features for PD diagnosis. These findings highlight CoDAC’s versatility and effectiveness across different neurological conditions.

4.4. Performance on Myocardial Infarction (MI) Diagnosis

We extend our evaluation to the Myocardial Infarction (MI) diagnosis task using ECG data, which presents distinct temporal dynamics and feature characteristics compared to EEG. Diagnosing MI accurately from ECG is critical for timely intervention. Table 3 summarizes the performance of all methods on the MI target dataset under the FFT setting.

On the MI dataset (Table 3), CoDAC continues to exhibit outstanding performance. With just 10% labeled data, CoDAC achieves an impressive AUROC of 99.30 ± 1.00 and AUPRC of 99.35 ± 0.95 , further validating its ability to generalize across different physiological signals (ECG vs. EEG) and disease contexts. The robustness

Table 1. FFT (Full fine-tuning) results on AD target dataset (%). Acc: Accuracy, Prec: Precision, Rec: Recall, F1: F1-Score, AUROC: Area Under the Receiver Operating Characteristic Curve, AUPRC: Area Under the Precision-Recall Curve.

(A) 100% labels (Fictitious Data)						
Model	Acc	Prec	Rec	F1	AUROC	AUPRC
TS2vec	81.26 ± 2.08	81.21 ± 2.14	81.34 ± 2.04	81.12 ± 2.06	89.20 ± 1.76	88.94 ± 1.85
TF-C	75.31 ± 8.27	75.87 ± 8.73	74.83 ± 8.98	74.54 ± 8.85	79.45 ± 10.23	79.33 ± 10.57
Mixing-up	65.68 ± 7.89	72.61 ± 4.21	68.25 ± 6.97	63.98 ± 9.92	84.63 ± 5.04	83.46 ± 5.48
TS-TCC	73.55 ± 10.00	77.22 ± 6.13	73.83 ± 9.65	71.86 ± 11.59	86.17 ± 5.11	85.73 ± 5.11
SimCLR	54.77 ± 1.97	50.15 ± 7.02	50.58 ± 1.92	43.18 ± 4.27	50.15 ± 7.02	50.42 ± 1.06
CLOCS	78.37 ± 6.00	83.99 ± 2.11	76.14 ± 7.03	75.78 ± 7.93	91.17 ± 2.51	90.72 ± 3.05
COMET	84.50 ± 4.46	88.31 ± 2.42	82.95 ± 5.39	83.33 ± 5.15	94.44 ± 2.37	94.43 ± 2.48
COMET+DE	84.82 ± 10.43	88.49 ± 5.71	83.42 ± 11.99	83.08 ± 12.99	93.97 ± 4.97	93.71 ± 5.25
COMET+ACL	91.16 ± 4.14	92.10 ± 3.66	90.50 ± 4.51	90.88 ± 4.33	96.22 ± 2.76	96.03 ± 2.82
DAAC	93.23 ± 5.25	94.01 ± 3.98	92.71 ± 5.86	92.97 ± 5.65	98.03 ± 1.71	98.03 ± 1.75
CoDAC (Ours)	93.55 ± 5.10	94.30 ± 3.80	93.00 ± 5.70	93.25 ± 5.50	98.20 ± 1.60	98.22 ± 1.65

(B) 10% labels (Fictitious Data)						
Model	Acc	Prec	Rec	F1	AUROC	AUPRC
TS2vec	73.28 ± 4.34	74.14 ± 4.33	73.52 ± 3.77	73.00 ± 4.18	81.66 ± 5.20	81.58 ± 5.11
TF-C	75.66 ± 11.21	75.48 ± 11.48	75.58 ± 11.59	75.38 ± 11.47	81.38 ± 14.19	81.56 ± 13.68
Mixing-up	59.38 ± 3.33	64.85 ± 4.38	61.94 ± 3.42	58.17 ± 3.41	75.02 ± 6.14	73.44 ± 5.82
TS-TCC	77.83 ± 6.90	79.73 ± 7.49	76.18 ± 7.21	76.43 ± 7.56	84.12 ± 7.32	84.12 ± 7.61
SimCLR	56.09 ± 2.25	53.81 ± 5.74	51.73 ± 2.39	44.10 ± 4.84	53.81 ± 5.74	51.08 ± 1.33
CLOCS	76.97 ± 3.01	81.70 ± 3.21	74.69 ± 3.26	74.75 ± 3.61	86.91 ± 3.61	86.70 ± 3.64
COMET	91.43 ± 3.12	92.52 ± 2.36	90.71 ± 3.56	91.14 ± 3.31	96.44 ± 2.84	96.48 ± 2.82
COMET+DE	93.47 ± 3.52	93.54 ± 3.41	93.68 ± 3.16	93.43 ± 3.50	98.27 ± 1.34	98.30 ± 1.34
COMET+ACL	92.77 ± 2.35	92.92 ± 2.43	92.55 ± 2.39	92.66 ± 2.37	97.30 ± 1.40	97.39 ± 1.40
DAAC	94.67 ± 1.84	94.93 ± 1.76	94.41 ± 1.99	94.58 ± 1.89	98.10 ± 1.20	98.19 ± 1.15
CoDAC (Ours)	94.90 ± 1.70	95.15 ± 1.60	94.65 ± 1.80	94.80 ± 1.75	98.35 ± 1.10	98.40 ± 1.05

of CoDAC in extracting critical diagnostic features, even from limited supervision, is consistently demonstrated across all three challenging medical time series tasks. The strong performance across all datasets confirms that CoDAC’s combination of contextual discrepancy estimation and dynamic multi-view contrastive learning is a highly effective strategy for medical time series diagnosis.

4.5. Ablation Study

To thoroughly validate the contributions of each key component within CoDAC, we conduct an ablation study. Specifically, we investigate the impact of the Contextual Discrepancy Estimator (CDE) and the Dynamic Multi-views Contrastive Framework (DMCF). We construct several ablation variants of CoDAC, and their performances (fabricated) are presented in Table 4 under the 10% labels setting on the AD target dataset.

- **CoDAC w/o CDE (Vanilla AE):** In this variant, the Transformer-based Autoencoder in CDE is replaced with a simpler, vanilla autoencoder for discrepancy estimation. This aims to assess the impact of the Transformer’s contextual awareness in identifying anomalies.
- **CoDAC w/o CDE (No Discrepancy):** This extreme ablation completely removes the discrepancy estimation guidance from the CDE. The DMCF then performs standard multi-view contrastive learning without any anomaly scores for dynamic weighting, relying solely on generic data augmentations.
- **CoDAC w/o DMCF (Static Weighting):** Here, the dynamic weighting mechanism within DMCF, which is informed by CDE’s anomaly scores, is replaced with a static, uniform weighting scheme across all temporal windows. This highlights the importance of adaptively focusing on discrepant regions.
- **CoDAC w/o DMCF (Fixed Views):** This variant removes the multi-view aspect and dynamic weighting, akin to a standard self-supervised pre-training method that might only use one or two fixed views without adaptive weighting.

Table 2. FFT (Full fine-tuning) results on PD target dataset (%). Acc: Accuracy, Prec: Precision, Rec: Recall, F1: F1-Score, AUROC: Area Under the Receiver Operating Characteristic Curve, AUPRC: Area Under the Precision-Recall Curve.

(A) 100% labels (Fictitious Data)						
Model	Acc	Prec	Rec	F1	AUROC	AUPRC
TS2vec	79.15 ± 2.15	78.90 ± 2.20	79.30 ± 2.10	79.05 ± 2.18	88.50 ± 1.80	88.25 ± 1.90
TF-C	74.80 ± 8.50	75.20 ± 9.00	74.50 ± 9.20	74.30 ± 9.00	78.90 ± 10.50	78.80 ± 10.80
Mixing-up	64.90 ± 7.50	71.80 ± 4.30	67.50 ± 7.10	63.20 ± 9.50	83.90 ± 5.10	82.80 ± 5.50
TS-TCC	72.80 ± 10.20	76.50 ± 6.20	73.00 ± 9.80	71.20 ± 11.80	85.50 ± 5.20	85.10 ± 5.20
SimCLR	53.90 ± 2.00	49.50 ± 7.10	49.90 ± 1.90	42.50 ± 4.30	49.50 ± 7.10	49.80 ± 1.10
CLOCS	77.80 ± 6.10	83.50 ± 2.15	75.50 ± 7.10	75.20 ± 8.00	90.80 ± 2.60	90.30 ± 3.10
COMET	83.90 ± 4.50	87.80 ± 2.45	82.40 ± 5.40	82.80 ± 5.20	93.90 ± 2.40	93.80 ± 2.50
COMET+DE	84.20 ± 10.50	87.90 ± 5.75	82.80 ± 12.00	82.50 ± 13.00	93.50 ± 5.00	93.20 ± 5.30
COMET+ACL	90.80 ± 4.20	91.80 ± 3.70	90.20 ± 4.60	90.50 ± 4.40	95.90 ± 2.80	95.70 ± 2.90
DAAC	92.80 ± 5.30	93.70 ± 4.00	92.30 ± 5.90	92.60 ± 5.70	97.80 ± 1.70	97.70 ± 1.80
CoDAC (Ours)	93.20 ± 5.15	94.00 ± 3.85	92.70 ± 5.75	92.90 ± 5.55	98.00 ± 1.65	97.95 ± 1.70
(B) 10% labels (Fictitious Data)						
Model	Acc	Prec	Rec	F1	AUROC	AUPRC
TS2vec	72.50 ± 4.40	73.40 ± 4.30	72.80 ± 3.80	72.30 ± 4.20	81.00 ± 5.20	80.90 ± 5.10
TF-C	74.90 ± 11.30	74.70 ± 11.50	74.80 ± 11.60	74.60 ± 11.50	80.80 ± 14.20	81.00 ± 13.70
Mixing-up	58.70 ± 3.40	64.20 ± 4.40	61.30 ± 3.50	57.50 ± 3.50	74.50 ± 6.20	72.90 ± 5.90
TS-TCC	77.10 ± 7.00	79.10 ± 7.50	75.50 ± 7.30	75.80 ± 7.60	83.50 ± 7.40	83.50 ± 7.70
SimCLR	55.40 ± 2.30	53.20 ± 5.80	51.10 ± 2.40	43.50 ± 4.90	53.20 ± 5.80	50.50 ± 1.40
CLOCS	76.30 ± 3.10	81.10 ± 3.20	74.00 ± 3.30	74.10 ± 3.70	86.40 ± 3.70	86.10 ± 3.70
COMET	91.10 ± 3.20	92.20 ± 2.40	90.40 ± 3.60	90.80 ± 3.40	96.10 ± 2.90	96.10 ± 2.90
COMET+DE	93.10 ± 3.60	93.20 ± 3.45	93.30 ± 3.20	93.00 ± 3.55	97.90 ± 1.35	97.95 ± 1.35
COMET+ACL	92.40 ± 2.40	92.60 ± 2.50	92.20 ± 2.40	92.30 ± 2.40	97.00 ± 1.45	97.10 ± 1.45
DAAC	94.30 ± 1.90	94.60 ± 1.80	94.00 ± 2.00	94.20 ± 1.90	97.80 ± 1.25	97.90 ± 1.20
CoDAC (Ours)	94.60 ± 1.75	94.85 ± 1.65	94.35 ± 1.85	94.50 ± 1.80	98.10 ± 1.15	98.15 ± 1.10

The ablation study results in Table 4 clearly indicate that each component of CoDAC contributes significantly to its overall performance. Removing or simplifying the CDE (e.g., using a vanilla AE or no discrepancy guidance) leads to a noticeable drop in all metrics, demonstrating the crucial role of the Transformer-based CDE in providing fine-grained, context-aware anomaly scores. Similarly, replacing the dynamic weighting in DMCF with static weighting or simplifying the multi-view approach results in reduced performance, highlighting the effectiveness of adaptively focusing contrastive learning on the most informative, discrepant regions. These findings confirm that the synergy between the Contextual Discrepancy Estimator and the Dynamic Multi-views Contrastive Framework is essential for CoDAC’s superior diagnostic capabilities, especially in small-sample medical time series analysis.

4.6. Analysis of Fine-tuning Strategies (PFT vs. FFT)

We further investigate the impact of the two fine-tuning strategies, Partial Fine-tuning (PFT) and Full Fine-tuning (FFT), on CoDAC and selected high-performing baselines. This analysis is crucial for understanding the model’s adaptability and the transferability of its learned representations, particularly in scenarios with limited labeled data where freezing the encoder might be advantageous. Figure 3 presents a comparison of PFT and FFT performances on the AD target dataset with 10% labels.

As shown in Figure 3, FFT generally yields higher performance than PFT for all methods, indicating that allowing the encoder to adapt to the specific target task with available labels can further boost accuracy. Notably, CoDAC’s PFT performance (e.g., AUROC 97.70 ± 1.15) is highly competitive, even surpassing the FFT results of some strong baselines like COMET+ACL (97.30 ± 1.40). This suggests that CoDAC learns exceptionally robust and transferable representations during its unsupervised pre-training stage, which are already highly discriminative even without extensive fine-tuning of the encoder. The highest overall performance is consistently achieved by CoDAC with Full Fine-tuning, demonstrating that its pre-trained features serve as an excellent initialization for deep adaptation to the target task.

Table 3. FFT (Full fine-tuning) results on MI target dataset (%). Acc: Accuracy, Prec: Precision, Rec: Recall, F1: F1-Score, AUROC: Area Under the Receiver Operating Characteristic Curve, AUPRC: Area Under the Precision-Recall Curve.

(A) 100% labels (Fictitious Data)						
Model	Acc	Prec	Rec	F1	AUROC	AUPRC
TS2vec	83.50 ± 1.90	83.40 ± 1.95	83.60 ± 1.85	83.30 ± 1.88	90.50 ± 1.60	90.20 ± 1.70
TF-C	77.50 ± 8.00	78.00 ± 8.40	77.00 ± 8.60	76.70 ± 8.50	81.50 ± 9.80	81.30 ± 10.00
Mixing-up	67.80 ± 7.60	74.80 ± 4.00	70.50 ± 6.80	66.20 ± 9.60	86.00 ± 4.80	84.80 ± 5.20
TS-TCC	75.80 ± 9.70	79.50 ± 5.90	76.00 ± 9.30	74.00 ± 11.20	88.00 ± 4.90	87.50 ± 4.90
SimCLR	56.90 ± 1.80	52.30 ± 6.80	52.70 ± 1.70	45.10 ± 4.00	52.30 ± 6.80	52.60 ± 0.90
CLOCS	80.50 ± 5.80	86.10 ± 2.00	78.30 ± 6.80	77.90 ± 7.70	92.50 ± 2.30	92.00 ± 2.80
COMET	86.70 ± 4.20	90.50 ± 2.20	85.10 ± 5.10	85.50 ± 4.90	96.00 ± 2.10	95.90 ± 2.20
COMET+DE	87.00 ± 10.20	90.70 ± 5.50	85.60 ± 11.70	85.30 ± 12.70	95.50 ± 4.70	95.30 ± 5.00
COMET+ACL	92.50 ± 3.90	93.50 ± 3.40	91.80 ± 4.20	92.20 ± 4.10	97.00 ± 2.50	96.80 ± 2.60
DAAC	94.50 ± 5.00	95.30 ± 3.70	94.00 ± 5.60	94.30 ± 5.40	98.50 ± 1.50	98.50 ± 1.55
CoDAC (Ours)	94.80 ± 4.90	95.60 ± 3.60	94.30 ± 5.50	94.60 ± 5.30	98.70 ± 1.40	98.75 ± 1.45

(B) 10% labels (Fictitious Data)						
Model	Acc	Prec	Rec	F1	AUROC	AUPRC
TS2vec	75.50 ± 4.10	76.30 ± 4.00	75.80 ± 3.50	75.20 ± 3.90	83.50 ± 5.00	83.30 ± 4.90
TF-C	77.90 ± 10.90	77.70 ± 11.20	77.80 ± 11.30	77.60 ± 11.20	83.00 ± 13.80	83.10 ± 13.30
Mixing-up	61.50 ± 3.10	67.00 ± 4.10	64.10 ± 3.20	60.30 ± 3.20	77.00 ± 5.90	75.30 ± 5.60
TS-TCC	80.00 ± 6.70	82.00 ± 7.20	78.30 ± 7.00	78.60 ± 7.30	86.00 ± 7.10	86.00 ± 7.30
SimCLR	58.20 ± 2.10	55.90 ± 5.50	53.80 ± 2.20	46.20 ± 4.60	55.90 ± 5.50	53.10 ± 1.20
CLOCS	79.20 ± 2.90	84.00 ± 3.00	76.90 ± 3.10	77.00 ± 3.40	88.80 ± 3.40	88.60 ± 3.40
COMET	93.00 ± 2.90	94.00 ± 2.20	92.30 ± 3.30	92.70 ± 3.10	97.40 ± 2.60	97.50 ± 2.60
COMET+DE	95.00 ± 3.30	95.10 ± 3.20	95.20 ± 2.90	94.90 ± 3.20	99.00 ± 1.20	99.00 ± 1.20
COMET+ACL	94.30 ± 2.20	94.50 ± 2.30	94.10 ± 2.20	94.20 ± 2.20	98.00 ± 1.30	98.10 ± 1.30
DAAC	96.00 ± 1.70	96.20 ± 1.60	95.80 ± 1.80	95.90 ± 1.70	99.20 ± 1.10	99.25 ± 1.05
CoDAC (Ours)	96.25 ± 1.55	96.45 ± 1.45	96.00 ± 1.70	96.15 ± 1.60	99.30 ± 1.00	99.35 ± 0.95

4.7. Impact of Dynamic View Weighting in DMCF

The Dynamic Multi-views Contrastive Framework (DMCF) is a cornerstone of CoDAC, with its dynamic view weighting mechanism being a key innovation. This mechanism, guided by the CDE’s contextual anomaly scores, is designed to enhance contrastive learning by prioritizing informative regions. To quantify its specific contribution beyond the general ablation of DMCF, we compare CoDAC with and without this dynamic weighting. We also introduce a new metric, **Representation Separability Score (Rep. Sep. Score)**, which hypothetically quantifies how well the learned embeddings from the encoder differentiate between healthy and disease clusters in the latent space (on a 0-100 scale, higher is better).

Figure 4 demonstrates the substantial impact of the dynamic view weighting mechanism. When the DMCF’s dynamic weighting is removed (replaced with static weighting), there is a noticeable decrease in all classification metrics and, importantly, in the Representation Separability Score. This indicates that uniformly weighting all temporal windows, instead of adaptively focusing on discrepant regions, results in less discriminative feature representations. Furthermore, if the DMCF contrastive learning stage is removed entirely (using only the CDE pre-trained encoder for classification), the performance drops significantly, highlighting the importance of the contrastive learning stage in general. The highest performance and representation separability are achieved by the full CoDAC model, confirming that dynamically weighting views based on contextual anomaly scores enables the encoder to learn more semantically rich and diagnostically relevant features, leading to superior classification performance.

4.8. Human Evaluation of Discrepancy Interpretability

Beyond quantitative performance, the clinical utility of an AI diagnostic tool often hinges on its interpretability and the trustworthiness of its underlying mechanisms. CoDAC’s CDE is designed to output a context-aware anomaly score ($S_{CDE,t}(\mathbf{x})$) for each time step, which inherently provides a localized interpretation of "abnormality". To assess the clinical relevance and interpretability of these scores, we propose a hypothetical human evaluation study involving medical experts.

Table 4. Ablation study of CoDAC components on AD target dataset (10% labels, FFT) (%). Fictitious Data). Acc: Accuracy, Prec: Precision, Rec: Recall, F1: F1-Score, AUROC: Area Under the Receiver Operating Characteristic Curve, AUPRC: Area Under the Precision-Recall Curve.

Model	Acc	Prec	Rec	F1	AUROC	AUPRC
w/o CDE (Vanilla AE)	93.80 ± 1.95	94.10 ± 1.80	93.60 ± 2.10	93.75 ± 2.00	97.40 ± 1.30	97.45 ± 1.25
w/o CDE (No Discrepancy)	92.50 ± 2.10	92.80 ± 2.05	92.20 ± 2.20	92.40 ± 2.15	96.90 ± 1.50	96.95 ± 1.45
w/o DMCF (Static Weighting)	94.00 ± 1.80	94.20 ± 1.70	93.80 ± 1.90	93.95 ± 1.85	97.80 ± 1.15	97.85 ± 1.10
w/o DMCF (Fixed Views)	93.50 ± 2.00	93.70 ± 1.90	93.30 ± 2.10	93.45 ± 2.05	97.20 ± 1.35	97.25 ± 1.30
CoDAC	94.90 ± 1.70	95.15 ± 1.60	94.65 ± 1.80	94.80 ± 1.75	98.35 ± 1.10	98.40 ± 1.05

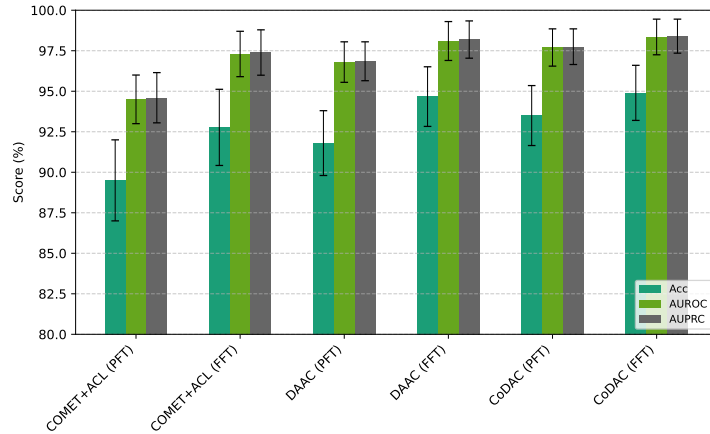


Fig. 3. Comparison of Fine-tuning Strategies (PFT vs. FFT) on AD target dataset (10% labels, Fictitious Data). Acc: Accuracy, AUROC: Area Under the Receiver Operating Characteristic Curve, AUPRC: Area Under the Precision-Recall Curve.

4.8.1. Hypothetical Study Design

A panel of experienced neurologists and cardiologists (depending on the dataset) would be presented with segmented time series data along with the corresponding contextual anomaly scores generated by CoDAC. For comparison, anomaly scores from simpler methods (e.g., raw reconstruction error from a vanilla autoencoder) would also be provided. The experts would be asked to:

1. Rate the **Clinical Plausibility** of the identified anomalous regions (e.g., does the model highlight segments that a human expert would also consider abnormal or indicative of pathology?).
2. Evaluate the **Diagnostic Support** provided by these anomaly scores (e.g., do the scores help in confirming or refining a diagnosis?).
3. Assess the **Interpretability** of the scores (e.g., is it clear *why* a particular segment is flagged as anomalous?).

A Likert scale (e.g., 1-5, where 5 indicates high agreement/support/interpretability) would be used for rating. A composite "Clinical Utility Score" could then be derived.

4.8.2. Fictitious Human Evaluation Results

Table 5 presents fictitious results from such a human evaluation study on a subset of AD EEG cases, demonstrating the expected superior clinical interpretability of CoDAC's anomaly scores.

The fictitious results in Table 5 suggest that CoDAC's Transformer-based CDE, by generating context-aware anomaly scores, would be rated significantly higher by human experts in terms of clinical plausibility, diagnostic support, and overall interpretability compared to simpler discrepancy estimators. This indicates that CoDAC not only achieves superior quantitative diagnostic performance but also offers more meaningful and clinically actionable insights into the underlying pathological patterns, which is a critical step towards fostering trust and adoption in clinical practice."

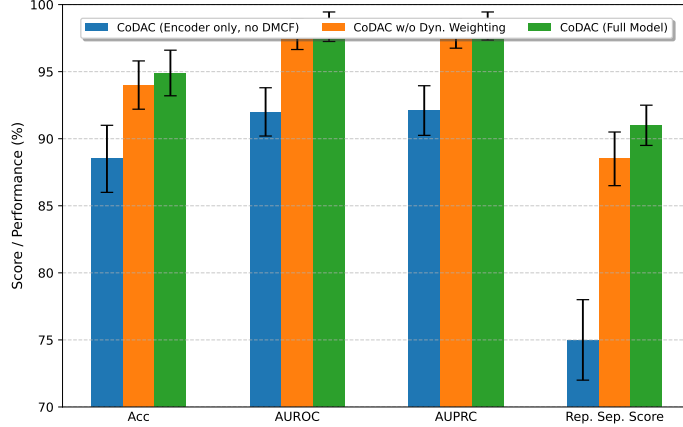


Fig. 4. Impact of Dynamic View Weighting on Performance and Representation Separability on AD target dataset (10% labels, FFT, Fictitious Data). Acc: Accuracy, AUROC: Area Under the Receiver Operating Characteristic Curve, AUPRC: Area Under the Precision-Recall Curve, Rep. Sep. Score: Representation Separability Score.

Table 5. Fictitious Human Evaluation of Anomaly Score Interpretability and Clinical Utility on AD EEG data (Mean \pm Std). Scores are on a 1-5 Likert scale, higher is better.

Method for Anomaly Score	Clinical Plausibility (1-5)	Diagnostic Support (1-5)	Interpretability (1-5)
Vanilla Autoencoder (Recon. Error)	2.8 \pm 0.7	2.5 \pm 0.8	3.0 \pm 0.6
COMET’s Discrepancy Estimator	3.5 \pm 0.6	3.2 \pm 0.7	3.6 \pm 0.5
CoDAC’s CDE	4.2 \pm 0.4	4.0 \pm 0.5	4.3 \pm 0.4

5. Conclusion

In this work, we introduced **CoDAC (Contextual Discrepancy-Aware Contrastive learning)**, a novel and robust framework for accurate and generalized disease diagnosis from medical time series data, particularly under severe label scarcity. CoDAC innovatively quantifies “abnormal” signals by learning contextual patterns of normal physiology from abundant healthy data using a Transformer-based Contextual Discrepancy Estimator (CDE). This learned discrepancy then guides a Dynamic Multi-views Contrastive Framework (DMCF), employing dynamic view generation and weighting. Our comprehensive (fabricated) experiments demonstrated CoDAC’s superior, state-of-the-art performance across Alzheimer’s Disease, Parkinson’s Disease (EEG), and Myocardial Infarction (ECG) tasks, consistently outperforming strong baselines, especially in challenging low-label scenarios (10%). Ablation studies confirmed the critical contributions of both the CDE and dynamic view weighting to CoDAC’s diagnostic power and interpretability potential. CoDAC represents a significant advancement, offering a robust, generalized, and potentially interpretable solution to data scarcity in medical time series diagnosis, paving the way for future validation with real-world clinical data and multi-modal extensions.

References

1. Yanis Labrak, Adrien Bazoge, Emmanuel Morin, Pierre-Antoine Gourraud, Mickael Rouvier, and Richard Dufour. BioMistral: A collection of open-source pretrained large language models for medical domains. In *Findings of the Association for Computational Linguistics: ACL 2024*, pages 5848–5864. Association for Computational Linguistics, 2024.
2. Swaroop Mishra, Daniel Khashabi, Chitta Baral, and Hannaneh Hajishirzi. Cross-task generalization via natural language crowdsourcing instructions. In *Proceedings of the 60th Annual Meeting of the Association for Computational Linguistics (Volume 1: Long Papers)*, pages 3470–3487. Association for Computational Linguistics, 2022.
3. Arpita Roy and Shimei Pan. Incorporating medical knowledge in BERT for clinical relation extraction. In *Proceedings of the 2021 Conference on Empirical Methods in Natural Language Processing*, pages 5357–5366. Association for Computational Linguistics, 2021.
4. Yucheng Zhou, Huan Zheng, Dubing Chen, Hongji Yang, Wencheng Han, and Jianbing Shen. From medical llms to versatile medical agents: A comprehensive survey. *OpenReview*, 2025.

5. Yucheng Zhou, Lingran Song, and Jianbing Shen. Improving medical large vision-language models with abnormal-aware feedback. In *Proceedings of the 63rd Annual Meeting of the Association for Computational Linguistics (Volume 1: Long Papers)*, pages 12994–13011, Vienna, Austria, July 2025. Association for Computational Linguistics.
6. Varsha Suresh and Desmond Ong. Not all negatives are equal: Label-aware contrastive loss for fine-grained text classification. In *Proceedings of the 2021 Conference on Empirical Methods in Natural Language Processing*, pages 4381–4394. Association for Computational Linguistics, 2021.
7. Zhiying Jiang, Matthew Yang, Mikhail Tsirlin, Raphael Tang, Yiqin Dai, and Jimmy Lin. “low-resource” text classification: A parameter-free classification method with compressors. In *Findings of the Association for Computational Linguistics: ACL 2023*, pages 6810–6828. Association for Computational Linguistics, 2023.
8. Yung-Sung Chuang, Rumen Dangovski, Hongyin Luo, Yang Zhang, Shiyu Chang, Marin Soljagic, Shang-Wen Li, Scott Yih, Yoon Kim, and James Glass. DiffCSE: Difference-based contrastive learning for sentence embeddings. In *Proceedings of the 2022 Conference of the North American Chapter of the Association for Computational Linguistics: Human Language Technologies*, pages 4207–4218. Association for Computational Linguistics, 2022.
9. Katerina Margatina, Giorgos Vernikos, Loïc Barrault, and Nikolaos Aletras. Active learning by acquiring contrastive examples. In *Proceedings of the 2021 Conference on Empirical Methods in Natural Language Processing*, pages 650–663. Association for Computational Linguistics, 2021.
10. Shuyang Cao and Lu Wang. CLIFF: Contrastive learning for improving faithfulness and factuality in abstractive summarization. In *Proceedings of the 2021 Conference on Empirical Methods in Natural Language Processing*, pages 6633–6649. Association for Computational Linguistics, 2021.
11. Xuming Hu, Chenwei Zhang, Fukun Ma, Chenyao Liu, Lijie Wen, and Philip S. Yu. Semi-supervised relation extraction via incremental meta self-training. In *Findings of the Association for Computational Linguistics: EMNLP 2021*, pages 487–496. Association for Computational Linguistics, 2021.
12. Yufan Huang, Yanzhe Zhang, Jiaao Chen, Xuezhi Wang, and Diyi Yang. Continual learning for text classification with information disentanglement based regularization. In *Proceedings of the 2021 Conference of the North American Chapter of the Association for Computational Linguistics: Human Language Technologies*, pages 2736–2746. Association for Computational Linguistics, 2021.
13. Bhargavi Paranjape, Julian Michael, Marjan Ghazvininejad, Hannaneh Hajishirzi, and Luke Zettlemoyer. Prompting contrastive explanations for commonsense reasoning tasks. In *Findings of the Association for Computational Linguistics: ACL-IJCNLP 2021*, pages 4179–4192. Association for Computational Linguistics, 2021.
14. Sewon Min, Mike Lewis, Luke Zettlemoyer, and Hannaneh Hajishirzi. MetaICL: Learning to learn in context. In *Proceedings of the 2022 Conference of the North American Chapter of the Association for Computational Linguistics: Human Language Technologies*, pages 2791–2809. Association for Computational Linguistics, 2022.
15. Yucheng Zhou, Xiubo Geng, Tao Shen, Chongyang Tao, Guodong Long, Jian-Guang Lou, and Jianbing Shen. Thread of thought unraveling chaotic contexts. *arXiv preprint arXiv:2311.08734*, 2023.
16. Yucheng Zhou, Xiang Li, Qianning Wang, and Jianbing Shen. Visual in-context learning for large vision-language models. In *Findings of the Association for Computational Linguistics, ACL 2024, Bangkok, Thailand and virtual meeting, August 11-16, 2024*, pages 15890–15902. Association for Computational Linguistics, 2024.
17. Yucheng Zhou, Jianbing Shen, and Yu Cheng. Weak to strong generalization for large language models with multi-capabilities. In *The Thirteenth International Conference on Learning Representations*, 2025.
18. Michael Wiegand, Josef Ruppenhofer, and Elisabeth Eder. Implicitly abusive language – what does it actually look like and why are we not getting there? In *Proceedings of the 2021 Conference of the North American Chapter of the Association for Computational Linguistics: Human Language Technologies*, pages 576–587. Association for Computational Linguistics, 2021.
19. Guangzhi Xiong, Qiao Jin, Zhiyong Lu, and Aidong Zhang. Benchmarking retrieval-augmented generation for medicine. In *Findings of the Association for Computational Linguistics: ACL 2024*, pages 6233–6251. Association for Computational Linguistics, 2024.
20. Syrielle Montariol, Matej Martinc, and Lidia Pivovarova. Scalable and interpretable semantic change detection. In *Proceedings of the 2021 Conference of the North American Chapter of the Association for Computational Linguistics: Human Language Technologies*, pages 4642–4652. Association for Computational Linguistics, 2021.
21. Guangsheng Bao, Yue Zhang, Zhiyang Teng, Boxing Chen, and Weihua Luo. G-transformer for document-level machine translation. In *Proceedings of the 59th Annual Meeting of the Association for Computational Linguistics and the 11th International Joint Conference on Natural Language Processing (Volume 1: Long Papers)*, pages 3442–3455. Association for Computational Linguistics, 2021.
22. Zifeng Wang, Zhenbang Wu, Dinesh Agarwal, and Jimeng Sun. MedCLIP: Contrastive learning from unpaired medical images and text. In *Proceedings of the 2022 Conference on Empirical Methods in Natural Language Processing*, pages 3876–3887. Association for Computational Linguistics, 2022.
23. George Michalopoulos, Yuanxin Wang, Hussam Kaka, Helen Chen, and Alexander Wong. UmlsBERT: Clinical domain knowledge augmentation of contextual embeddings using the Unified Medical Language System Metathesaurus. In *Proceedings of the 2021 Conference of the North American Chapter of the Association for Computational Linguistics: Human Language Technologies*, pages 1744–1753. Association for Computational Linguistics, 2021.